



相对论重离子对撞机上重味衰变电子的测量数据中粲和底成分的分离

司凡 陈小龙 张生辉 张一飞

Charm and Beauty Separation from Heavy Flavor Electron Measurements at RHIC

SI Fan, CHEN Xiaolong, ZHANG Shenghui, ZHANG Yifei

在线阅读 View online: <https://doi.org/10.11804/NuclPhysRev.37.2019CNPC13>

引用格式:

司凡, 陈小龙, 张生辉, 张一飞. 相对论重离子对撞机上重味衰变电子的测量数据中粲和底成分的分离[J]. 原子核物理评论, 2020, 37(3):684–689. doi: 10.11804/NuclPhysRev.37.2019CNPC13

SI Fan, CHEN Xiaolong, ZHANG Shenghui, ZHANG Yifei. Charm and Beauty Separation from Heavy Flavor Electron Measurements at RHIC[J]. Nuclear Physics Review, 2020, 37(3):684–689. doi: 10.11804/NuclPhysRev.37.2019CNPC13

您可能感兴趣的其他文章

Articles you may be interested in

[利用光前量子化方法计算电子的广义横向动量分布函数](#)

Investigation of the General Transverse Momentum Distribution Function in Light-front Wave Function Method

原子核物理评论. 2017, 34(4): 724–729 <https://doi.org/10.11804/NuclPhysRev.34.04.724>

[相对论重离子碰撞手征电荷分离效应的研究](#)

Study of Chiral Charge Separation Effect in Relativistic Heavy Ion Collisions

原子核物理评论. 2017, 34(3): 557–562 <https://doi.org/10.11804/NuclPhysRev.34.03.557>

[中能重离子碰撞中横向流电荷依赖的形状以及实验条件对横向流的影响\(英文\)](#)

Z-dependence Flow Pattern and Experimental Filter Effect on Transverse Flow Extraction in Intermediate-energy Heavy Ion Collisions

原子核物理评论. 2018, 35(1): 18–22 <https://doi.org/10.11804/NuclPhysRev.35.01.018>

[相对论重离子碰撞的输运模型研究](#)

Transport Model Studies on Relativistic Heavy-ion Collisions

原子核物理评论. 2017, 34(3): 370–373 <https://doi.org/10.11804/NuclPhysRev.34.03.370>

[高动量分布对核反应中原子核的阻止本领的影响](#)

Effect of High Momentum Distribution on Nuclear Stopping in Nuclear Reaction

原子核物理评论. 2017, 34(2): 143–147 <https://doi.org/10.11804/NuclPhysRev.34.02.143>

[格点核子-核子势在核物质中的相对论效应\(英文\)](#)

Relativistic Effects in Nuclear Matter with Lattice NN Potential

原子核物理评论. 2017, 34(3): 505–508 <https://doi.org/10.11804/NuclPhysRev.34.03.505>

Article ID: 1007-4627(2020)03-0684-06

Charm and Beauty Separation from Heavy Flavor Electron Measurements at RHIC

SI Fan, CHEN Xiaolong, ZHANG Shenghui, ZHANG Yifei[†]

(State Key Laboratory of Particle Detection and Electronics,
University of Science and Technology of China, Hefei 230026, China)

Abstract: Heavy quarks (charm and beauty), especially beauty, with expectedly different properties from light quarks are considered as ideal probes for the Quark-Gluon Plasma (QGP). However, there are few measurements on beauty hadrons or on their decay leptons. With the most recent measurements on charmed hadrons and heavy flavor decay electrons (HFE) at mid-rapidity in Au+Au collisions at $\sqrt{s_{NN}} = 200$ GeV at RHIC, a data-driven method is developed to separate charm and beauty components from the HFE measurements. From charmed hadron measurements, electrons from charm decays via semileptonic decay simulations are obtained, with which the beauty component can be extracted from the HFE spectrum. As preliminary results, the p_T spectra, R_{AA} and v_2 distributions of electrons from charm and from beauty decays ($R_{AA}^{c \rightarrow e}$ and $v_2^{c \rightarrow e}$, $R_{AA}^{b \rightarrow e}$ and $v_2^{b \rightarrow e}$) in minimum bias Au+Au collisions are presented, respectively. Less suppression of $R_{AA}^{b \rightarrow e}$ is observed compared with that of $R_{AA}^{c \rightarrow e}$ at moderate-to-high p_T , and $v_2^{b \rightarrow e}$ shows smaller than $v_2^{c \rightarrow e}$ at low-to-moderate p_T .

Key words: charm; beauty; electron; transverse momentum; nuclear modification factor; elliptic flow

CLC number: O572.2

Document code: A

DOI: [10.11804/NuclPhysRev.37.2019CNPC13](https://doi.org/10.11804/NuclPhysRev.37.2019CNPC13)

1 Introduction

The Quark-Gluon Plasma (QGP) is predicted by the Quantum Chromodynamics (QCD) as a new matter state containing deconfined quarks and gluons under extremely high temperature and density. It is believed to have been produced in the early universe after the Big Bang. Recent experimental results from the Relativistic Heavy-Ion Collider (RHIC) at Brookhaven National Laboratory (BNL) and the Large Hadron Collider (LHC) at European Organization for Nuclear Research (CERN) support that a strongly coupled QGP (sQGP) has been created in ultra-relativistic heavy-ion collisions, mimicking the early universe^[1-2]. To study the properties of the QGP and its evolution is particularly helpful for understanding the early universe.

Charm and beauty are called as heavy quarks due to their much larger masses compared to those of light

quarks (u, d and s). Heavy quarks are believed to be created predominantly via initial hard scatterings before the formation of the QGP in the early stage of heavy-ion collisions^[3-4], and to experience the full time evolution of the QGP. Their total yields can be evaluated by the perturbative-QCD (pQCD) theory and be scaled with the number of binary collisions (N_{coll})^[4]. For these reasons, heavy quarks are always considered as ideal probes for studying the properties of the QGP.

When partons travel inside the hot-dense medium and interact with the medium constituents, they deposit energy into the medium. Theoretical calculations predict that the radiative part of the partonic energy loss is mass dependent^[5]. The energy loss of heavy quarks should be smaller than that of light quarks due to the suppression of the gluon radiation in the forward angle by the quark mass, and beauty would lose even less energy than charm for it is three

Received date: 15 Dec. 2019; **Revised date:** 21 Feb. 2020

Foundation item: National Key R&D Program of China (2018YFE0205200); National Natural Science Foundation of China (11890712); Anhui Provincial Natural Science Foundation (1808085J02); Fundamental Research Funds for the Central Universities (WK2030000013); China Postdoctoral Science Foundation (2019M652177)

Biography: SI Fan(1998-), male, Kaifeng, Henan, Postgraduate, working on the particle physics and nuclear physics; E-mail: sifan98@mail.ustc.edu.cn

† Corresponding author: ZHANG Yifei, E-mail: ephy@ustc.edu.cn.

times heavier than charm quark. The heavy quark production as a function of the transverse momentum (p_T) is predicted to be modified by their energy loss^[6], which, experimentally, is usually characterized by the nuclear modification factor (R_{AA})^[7] defined as

$$R_{AA}(p_T) = \frac{1}{\langle N_{\text{coll}} \rangle} \frac{dN_{AA}/dp_T}{dN_{pp}/dp_T}, \quad (1)$$

where dN_{AA}/dp_T and dN_{pp}/dp_T are particle production yields in A+A and p+p collisions, respectively, and $\langle N_{\text{coll}} \rangle$ is the average N_{coll} often calculated using a Monte Carlo Glauber model. The dN_{pp}/dp_T is used as the baseline since there is no QGP created in p+p collisions. With the normalization of $\langle N_{\text{coll}} \rangle$, R_{AA} should be equal to unity if there is no medium effect in A+A collisions. Partonic energy loss could result in a suppression on the value of R_{AA} at moderate-to-high p_T . Recent measurements on the R_{AA} of open charm hadrons show strong suppression at high p_T with a similar magnitude as light flavor hadrons, suggesting significant interactions between charm and the sQGP medium^[8]. However, most of heavy flavor electron (HFE) measurements report results on electrons from heavy flavor decays without charm and beauty components separated due to technique limits, and large uncertainties are reported in a few existing separations for these two components^[9].

An anisotropic collectivity exists in the expanding medium created in heavy-ion collisions^[10]. Light quarks are unable to prevent themselves from following the collective flow and achieving thermal equilibrium^[11]. However, heavy quarks are expected to be more difficult to mobilize and to obtain anisotropic momenta because of their much larger masses. To describe the azimuthal anisotropy, a Fourier expansion of the azimuthal angle (φ) is obtained in the momentum space as^[12]

$$E \frac{d^3N}{d^3p} = \frac{d^2N}{2\pi p_T dp_T dy} \left\{ 1 + \sum_{n=1}^{\infty} 2v_n \cos [n(\varphi - \psi_R)] \right\}, \quad (2)$$

where ψ_R denotes the reaction plane (defined by the beam axis and the direction of the impact parameter between two colliding nuclei). And the elliptic flow (v_2) is defined as the 2nd coefficient

$$v_2(p_T) = \langle \cos [2(\varphi - \psi_R)] \rangle. \quad (3)$$

The heavy quark v_2 is proposed to be a significant observable for quantifying partonic matter properties, such as the thermalization^[6]. Recent measurements shows that charm gains significant flow like light

quarks through interactions with the sQGP medium^[13]. Because beauty is three times heavier than charm, its behavior in the anisotropic collective flow could be different from that of charm. However, most of heavy flavor v_2 measurements are for charmed hadrons or the HFE and there are few results for beauty v_2 via either hadronic decays or semileptonic channels at RHIC.

2 Data-driven method

We have developed a data-driven method to separate charm and beauty components from the HFE measurements on p_T spectra and on R_{AA} and v_2 distributions based on the most recent charmed hadron measurements at mid-rapidity in minimum bias (Min bias) Au+Au collisions at $\sqrt{s_{\text{NN}}} = 200 \text{ GeV}$ at RHIC. Parts of heavy flavor hadrons decay to light flavor hadrons and leptons, such as electrons, via semileptonic channels. These electrons carry information about the properties of origin heavy quarks.

It is started from the charmed hadron measurements on p_T spectra of D^0 ^[8], D^\pm ^[14], D_s ^[14], Λ_c ^[15] and J/ψ ^[16-17] at mid-rapidity in Au+Au collisions at $\sqrt{s_{\text{NN}}} = 200 \text{ GeV}$ with the STAR experiment at RHIC, all of which are parameterized and shown with uncertainty bands in Fig. 1. Measurements on D^0 at 0~80%, D_s at 10%~40% and J/ψ at 0~60% are used because of their largest statistics and best precision, and they are parameterized and extrapolated to $0 < p_T < 20 \text{ GeV}/c$ with the Levy function^[18]

$$\frac{d^2N}{2\pi p_T dp_T dy} = \frac{1}{2\pi} \frac{dN}{dy} \frac{(n-1)(n-2)}{nT[nT + m_0(n-2)]} \times \left(1 + \frac{\sqrt{p_T^2 + m_0^2} - m_0}{nT} \right)^{-n}, \quad (4)$$

and the power-law function^[19]

$$\frac{d^2N}{2\pi p_T dp_T dy} = \frac{2}{\pi} \frac{dN}{dy} \frac{(n-1)(n-2)}{(n-3)^2 \langle p_T \rangle^2} \times \left(1 + \frac{2p_T}{\langle p_T \rangle (n-3)} \right)^{-n}, \quad (5)$$

where m_0 is the rest mass of the particle. Halves of the differences between Levy and power-law fits are quadratically summed into uncertainty bands. The D^\pm spectrum is obtained by scaling the D^0 spectrum with a constant (0.429 ± 0.038) fitted from the D^\pm/D^0 ratio measured at 0~10% centrality, since there is no obverse p_T dependence observed. Because D^0 and D^\pm make up the triplet state of D-mesons, their properties, including shapes of the p_T spectra, should be

highly consistent. The Λ_c spectrum is fitted and extrapolated to the p_T range of 0~10 GeV/ c with the measured D^0 spectrum multiplied by the average of different model calculations on Λ_c/D^0 ratio: Ko^[20], Greco^[21] and Tshingua^[22] with their differences as the uncertainty.

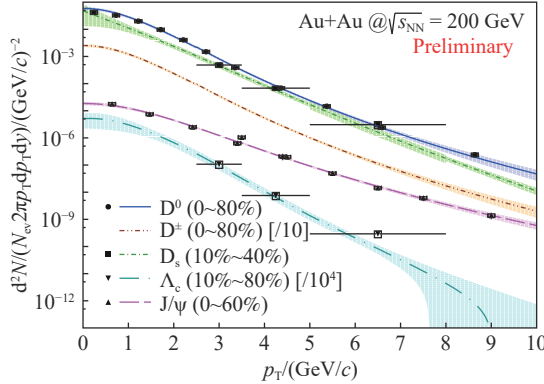


Fig. 1 (color online) Measured and parameterized p_T spectra with uncertainty bands of charmed hadrons (D^0 ^[8], D^\pm ^[14], D_s ^[14], Λ_c ^[15], J/ψ ^[16-17]) at mid-rapidity in Au+Au collisions at $\sqrt{s_{NN}} = 200$ GeV.

All aforementioned parameterized p_T spectra of charmed hadrons are input into Monte Carlo simulations of semileptonic decays to electrons, of which the J/ψ spectrum is input in a Pythia decayer^[23] decaying to e^+e^- . In each simulated event, we sample the hadron p_T from a uniform distribution with $\frac{dN}{dp_T}$ in this p_T bin as the weight in order to increase the statistics at higher p_T . The 4-momentum is determined additionally with a uniformly distributed azimuthal angle φ , a gaussian mid-rapidity y and the hadron mass. And the electron momentum in the hadron rest frame is sampled from the measured distribution^[24]. After Lorentz transformation, the final electron p_T from semileptonic decays in the laboratory frame can be obtained. The output electrons are filled in the $\frac{dN}{2\pi p_T dp_T}$ distribution. Upper and lower hadron spectrum uncertainties are also input into the simulations and propagated to the output accordingly.

The output electron p_T spectra are normalized by measured cross sections of parent hadrons and semileptonic decay branching ratios. In particular, those from D_s , Λ_c and J/ψ are scaled by N_{coll} to 0~80% centrality from 10%~40%, 10%~80% and 0~60%, respectively. Uncertainties of branching ratios, N_{coll} normalization (for D_s , Λ_c and J/ψ) and the D^\pm/D^0 ratio (for D^\pm) are also taken into account and propagated quadratically. Fig. 2 shows the final electron p_T spectra from charmed hadron decays and the summed charm component ($c \rightarrow e$) with shaded

bands as uncertainties at mid-rapidity in minimum bias Au+Au collisions at $\sqrt{s_{NN}} = 200$ GeV. The electron spectrum from beauty decays ($b \rightarrow e$) is calculated by subtracting the $c \rightarrow e$ component from the HFE spectrum measured by STAR^[25]. The $c \rightarrow e$ uncertainty contributions to the last two points of $b \rightarrow e$ at $p_T > 7$ GeV/ c are safely doubled due to higher p_T extrapolation of charmed hadron spectra.

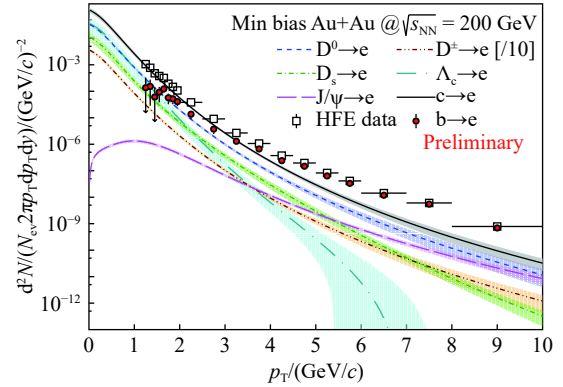


Fig. 2 (color online) Electron p_T spectra from charmed hadron decays and the sum of them ($c \rightarrow e$) with uncertainty bands at mid-rapidity in minimum bias Au+Au collisions at $\sqrt{s_{NN}} = 200$ GeV. The electron spectrum from beauty decays ($b \rightarrow e$) is obtained by subtracting $c \rightarrow e$ from the HFE data.

The beauty component fraction in the HFE spectrum is defined as

$$f^{b \rightarrow e} = \frac{dN^{b \rightarrow e}/dp_T}{dN^{\text{HFE}}/dp_T}. \quad (6)$$

Fig. 3 shows the $f^{b \rightarrow e}$ at mid-rapidity in minimum bias Au+Au collisions at $\sqrt{s_{NN}} = 200$ GeV ($f_{AA}^{b \rightarrow e}$) obtained from Fig. 2 compared with previous measure-

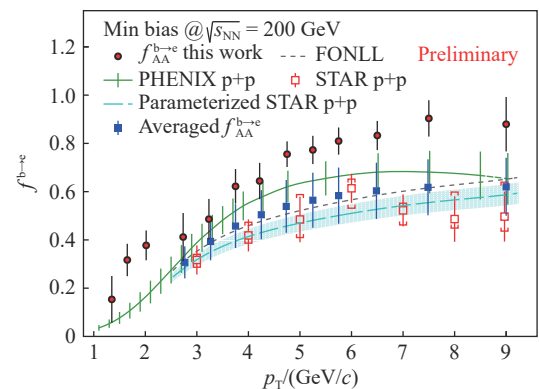


Fig. 3 (color online) Fractions of beauty decay electrons in the HFE ($f^{b \rightarrow e}$) at mid-rapidity in minimum bias Au+Au collisions at $\sqrt{s_{NN}} = 200$ GeV compared with the FONLL theoretical calculation^[4] and measurements by STAR^[26], by PHENIX^[27] and their average in p+p collisions. The last point of the PHENIX p+p data at 9 GeV/ c is extrapolated.

ments in p+p collisions ($f_{pp}^{b \rightarrow e}$) by STAR^[26] (red open squares) and by PHENIX^[27] (green crosses). The fixed-order next-to-leading log (FONLL) calculation^[4] is presented as the gray dashed curve, with which the STAR p+p data are parameterized (cyan dashed curve with band). Blue solid squares denote the average of the STAR and the PHENIX p+p data with half of their difference taken into account in the uncertainty bars. At $p_T \sim 3.5 \text{ GeV}/c$, beauty and charm components are comparable. The $f_{AA}^{b \rightarrow e}$ looks systematically higher than $f_{pp}^{b \rightarrow e}$, in particular in $p_T > 7 \text{ GeV}/c$ where $f_{AA}^{b \rightarrow e}$ increases up to $(90 \pm 10)\%$.

3 R_{AA} separation

The R_{AA} of electrons from charm and from beauty decays ($R_{AA}^{c \rightarrow e}$ and $R_{AA}^{b \rightarrow e}$) as functions of p_T can be extracted from the R_{AA} of the HFE (R_{AA}^{HFE}) measured by STAR^[25] with

$$R_{AA}^{c \rightarrow e} = \frac{1 - f_{AA}^{b \rightarrow e}}{1 - f_{pp}^{b \rightarrow e}} R_{AA}^{\text{HFE}}, \quad (7)$$

$$R_{AA}^{b \rightarrow e} = \frac{f_{AA}^{b \rightarrow e}}{f_{pp}^{b \rightarrow e}} R_{AA}^{\text{HFE}}, \quad (8)$$

which are shown as blue solid squares and red solid circles in Fig. 4, respectively. The $f_{pp}^{b \rightarrow e}$ here denotes the averaged one of STAR and PHENIX p+p data in Fig. 3. As a cross-check, two red dashed curves representing $b(c) \rightarrow e$ /FONLL are obtained directly by the definition of R_{AA} in Eq. (1) and show a good agreement with our results. Results of this work are con-

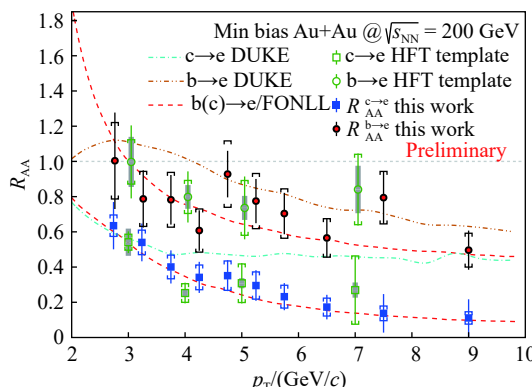


Fig. 4 (color online) The nuclear modification factors (R_{AA}) of $c \rightarrow e$ and $b \rightarrow e$ with HFT template analysis^[9] and DUKE model predictions^[28] as comparisons at mid-rapidity in minimum bias Au+Au collisions at $\sqrt{s_{NN}} = 200 \text{ GeV}$. Uncertainty bars of this work denote quadratically summed contributions of $f_{AA}^{b(c) \rightarrow e}$ and R_{AA}^{HFE} and boxes are from $f_{pp}^{b \rightarrow e}$. $b(c) \rightarrow e$ /FONLL are obtained directly with the R_{AA} definition.

sistent with the HFT template analysis (open green symbols)^[9] and show improved precision. The $R_{AA}^{b \rightarrow e}$ result is consistent with the DUKE model prediction^[28], but $R_{AA}^{c \rightarrow e}$ is clearly lower than the prediction in $p_T > 4 \text{ GeV}/c$. Less suppression of $R_{AA}^{b \rightarrow e}$ compared with that of $R_{AA}^{c \rightarrow e}$ can be observed, which could indicate the possible mass dependence of the energy loss of charm and beauty.

4 v_2 separation

The D^0 v_2 at 0~80% centrality measured by STAR^[13] is parameterized by Eq. (9)^[29] with the linear term forced to pass through the origin according to the properties of v_2 ,

$$v_2(p_T) = \frac{p_0 n}{1 + \exp\left(\frac{p_1 - \frac{p_T}{n}}{p_2}\right)} - \frac{p_0 n}{1 + \exp\left(\frac{p_1}{p_2}\right)} - p_3 n p_T, \quad (9)$$

where n is the number of constituent quarks, p_i ($i = 0, 1, 2, 3$) are free parameters. The v_2 distributions of D -mesons ($n_{\text{quarks}} = 2$) and Λ_c ($n_{\text{quarks}} = 3$) are obtained with the number-of-constituent-quark (NCQ) scaling assumption^[29–30] as v_2/n vs. $(\sqrt{p_T^2 + m_0^2} - m_0)/n$ from the parameterized D^0 v_2 . Semileptonic decays of charmed hadrons are simulated with the hadron p_T spectra and v_2 distributions as inputs. Different from the simulations in Sec. 2, the azimuthal angle φ in each p_T bin is sampled from the distribution^[29]

$$\frac{dN}{d\varphi} = 1 + 2v_2 \cos(2\varphi). \quad (10)$$

The v_2 of $D \rightarrow e$ ($v_2^{D \rightarrow e}$) and $\Lambda_c \rightarrow e$ ($v_2^{\Lambda_c \rightarrow e}$) as functions of p_T can be obtained by fitting the output electron φ distributions with Eq. (10) in different p_T bins. The uncertainty bands of charmed hadron v_2 from parameterization are also input into the simulations and propagated to electron v_2 distributions.

The v_2 of $c \rightarrow e$ ($v_2^{c \rightarrow e}$) is an average of $v_2^{D \rightarrow e}$ and $v_2^{\Lambda_c \rightarrow e}$ with their relative production yields in Fig. 2 as weights. In a similar way, the v_2 of $b \rightarrow e$ ($v_2^{b \rightarrow e}$) can be extracted with

$$v_2^{b \rightarrow e} = \frac{v_2^{\text{HFE}} - (1 - f_{AA}^{b \rightarrow e}) v_2^{c \rightarrow e}}{f_{AA}^{b \rightarrow e}}, \quad (11)$$

where v_2^{HFE} denotes the v_2 of the HFE obtained by parameterizing the combined distribution measured by STAR^[25] and PHENIX^[31] with Eq. (9). Fig. 5 shows the results of $v_2^{c \rightarrow e}$ (blue solid squares) and $v_2^{b \rightarrow e}$ (red solid circles). As a comparison, the v_2 of $\phi \rightarrow e$ ($v_2^{\phi \rightarrow e}$) shown as red open squares is calculated in the same way with the ϕ -meson p_T spectrum^[32] and v_2 ^[33]

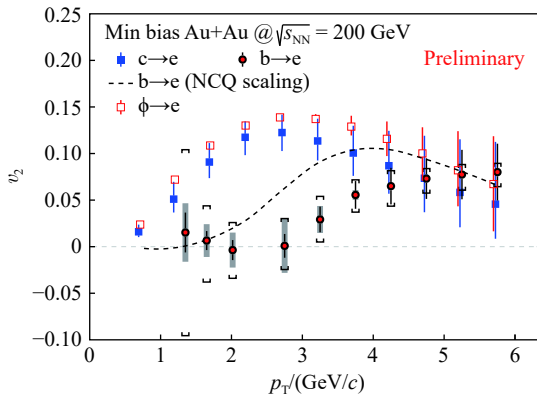


Fig. 5 (color online) The elliptic flows (v_2) of $c \rightarrow e$ and $b \rightarrow e$ at mid-rapidity in minimum bias Au+Au collisions at $\sqrt{s_{NN}} = 200$ GeV. The uncertainty of $v_2^{b \rightarrow e}$ is propagated from v_2^{HFE} (bars), $v_2^{c \rightarrow e}$ (brackets) and $f_{AA}^{b \rightarrow e}$ (grey bands). The $v_2^{b \rightarrow e}$ with the NCQ scaling assumption of the B-meson v_2 and $v_2^{\phi \rightarrow e}$ are shown as comparisons.

at 0~80% centrality as inputs of the Pythia decayer. A non-zero $v_2^{b \rightarrow e}$ in $p_T > 3.0 \text{ GeV}/c$ is observed and consistent with the electron v_2 from charmed and strange hadron decays within uncertainties in $p_T > 4.5 \text{ GeV}/c$. However, $v_2^{b \rightarrow e}$ is clearly smaller than $v_2^{c \rightarrow e}$ at $1.5 \text{ GeV}/c < p_T < 4.0 \text{ GeV}/c$. In addition, we unfold the B-meson p_T spectrum from the $b \rightarrow e$ points extracted in Fig. 2 and assume that the B-meson v_2 follows the NCQ scaling. The black dashed curve represents the refolded $v_2^{b \rightarrow e}$ with the Pythia decayer and our $v_2^{b \rightarrow e}$ result deviates from it at $2.5 \text{ GeV}/c < p_T < 4.5 \text{ GeV}/c$ with a confidence level of 98.2% ($\chi^2/ndf = 11.92/4$), which could be related to the beauty thermalization or its hadronization mechanism in the QGP.

5 Summary

This paper reports a data-driven method developed to separate charm and beauty components from heavy flavor electron measurements at mid-rapidity in minimum bias Au+Au collisions at RHIC. Semileptonic decays of charmed hadrons are simulated with the most recent measurements on charmed hadrons with RHIC-STAR as inputs. By subtracting the output electrons from charm decays, the beauty component is extracted from the HFE spectrum, and the p_T spectra, R_{AA} and v_2 distributions of electrons from charm and from beauty decays are obtained. In these preliminary results, less suppression of $R_{AA}^{b \rightarrow e}$ is observed than that of $R_{AA}^{c \rightarrow e}$ at moderate-to-high p_T , and $v_2^{b \rightarrow e}$ is smaller than $v_2^{c \rightarrow e}$, $v_2^{\phi \rightarrow e}$ and the $v_2^{b \rightarrow e}$ with the B-meson v_2 NCQ scaling assumption at low-to-moderate p_T . Improved results further elucidating

charm and beauty physics in heavy-ion collisions will be available in the near future.

References:

- [1] ADAMS J, AGGARWAL M M, AHAMMED Z, et al. *Nucl Phys A*, 2005, **757**(1-2): 102.
- [2] MULLER B, SCHUKRAFT J, WYSLOUCH B. *Ann Rev Nucl Part Sci*, 2012, **62**(1): 361.
- [3] LIN Z, GYULASSY M. *Phys Rev C*, 1995, **51**(4): 2177.
- [4] CACCIARI M, NASON P, VOGT R. *Phys Rev Lett*, 2005, **95**(12): 2001.
- [5] BUZZATTI A, GYULASSY M. *Phys Rev Lett*, 2012, **108**: 2301.
- [6] MOORE D G, TEANEY D. *Phys Rev C*, 2005, **71**(6): 4904.
- [7] WANG X, GYULASSY M. *Phys Rev Lett*, 1992, **68**(10): 1480.
- [8] ADAM J, ADAMCZYK L, ADAMS J, et al. *Phys Rev C*, 2019, **99**(3): 4908.
- [9] OH K. *Nucl Phys A*, 2017, **967**(1): 632.
- [10] ADAMS J, AGGARWAL M M, AHAMMED Z, et al. *Phys Rev C*, 2005, **72**(1): 4904.
- [11] ABELEV I B, AGGARWAL M M, AHAMMED Z, et al. *Phys Rev C*, 2008, **77**(5): 4901.
- [12] POSKANZER M A, VOLOSHIN A S. *Phys Rev C*, 1998, **58**(3): 1671.
- [13] ADAMCZYK L, ADKINS K J, AGAKISHIEV G, et al. *Phys Rev Lett*, 2017, **118**(21): 2301.
- [14] ZHOU L. *Nucl Phys A*, 2017, **967**(1): 620.
- [15] RADHAKRISHNAN S. *Nucl Phys A*, 2019, **982**(1): 659.
- [16] ADAMCZYK L, ADKINS K J, AGAKISHIEV G, et al. *Phys Rev C*, 2014, **90**(2): 4906.
- [17] ADAMCZYK L, AGAKISHIEV G, AGGARWAL M M, et al. *Phys Lett B*, 2013, **722**(1-3): 55.
- [18] WILK G, WLODARCZYK Z. *Phys Rev Lett*, 2000, **84**(13): 2770.
- [19] ADAMCZYK L, AGAKISHIEV G, AGGARWAL M M, et al. *Phys Rev D*, 2012, **86**(7): 2013.
- [20] LEE H S, OHNISHI K, YASUI S, et al. *Phys Rev Lett*, 2008, **100**(22): 2301.
- [21] GHOSH S, DAS K S, GRECO V, et al. *Phys Rev D*, 2014, **90**(5): 4018.
- [22] ZHAO J, SHI S, XU N, et al. arXiv: hep-ph/1805.10858.
- [23] SJÖSTRAND T, MRENNNA S, SKANDS P. *J High Energy Phys*, 2006, **2006**(5): 026.
- [24] LIU H, ZHANG Y, ZHONG C, et al. *Phys Lett B*, 2006, **639**(5): 441.
- [25] MUSTAFA M. *Nucl Phys A*, 2013, **904-905**(1): 665c.
- [26] AGGARWAL M M, AHAMMED Z, ALAKHVERDYANTS V A, et al. *Phys Rev Lett*, 2010, **105**(20): 2301.
- [27] AIDALA C, AKIBA Y, ALFRED M, et al. *Phys Rev D*, 2019, **99**(9): 2003.
- [28] CAO S, QIN G, BASS A S. *Phys Rev C*, 2015, **92**(2): 4907.
- [29] DONG X, ESUMI S, SORENSEN P, et al. *Phys Lett B*, 2004, **597**(3-4): 328.
- [30] TIAN J, CHEN J, MA Y, et al. *Phys Rev C*, 2009, **79**(6):

7901.

[31] HACHIYA T. *Nucl Phys A*, 2019, 982(1): 663.
[32] ABELEV I B, AGGARWAL M M, AHAMMED Z, *et al.*

Phys Rev Lett, 2007, 99(11): 2301.

[33] ADAMCZYK L, ADKINS K J, AGAKISHIEV G, *et al.* *Phys Rev Lett*, 2016, 116(6): 2301.

相对论重离子对撞机上重味衰变电子的测量数据中粲和底成分的分离

司凡, 陈小龙, 张生辉, 张一飞[†]

(核探测与核电子学国家重点实验室, 中国科学技术大学, 合肥 230026)

摘要: 重味夸克(即粲和底), 尤其是底夸克, 具有预期不同于轻夸克的性质, 被认为是夸克胶子等离子体的理想探针。然而, 很少有对底强子或其衰变的轻子的测量。利用最近相对论重离子对撞机上 $\sqrt{s_{NN}} = 200 \text{ GeV}$ 的金核-金核碰撞中产生于中心快度下的粲强子和重味衰变电子的测量数据, 我们发展了一种数据驱动的方法, 用于分离重味衰变电子中粲和底的成分。从粲强子的测量数据出发, 通过模拟其半轻子衰变到粲衰变电子, 从而从重味衰变电子中提取出底的成分。初步的结果展示了在最小偏向的金核-金核碰撞中粲和底衰变电子的横动量谱、核修正因子和椭圆流的分布。在中等至较高横动量区, 相比于粲衰变电子的核修正因子, 底衰变电子的核修正因子受到了较小的压制; 在较低至中等横动量区, 底衰变电子获得了比粲衰变电子更小的椭圆流。

关键词: 粲; 底; 电子; 横动量; 核修正因子; 椭圆流

收稿日期: 2019-12-15; 修改日期: 2020-02-21

基金项目: 国家重点研发计划项目(2018YFE0205200); 国家自然科学基金项目(11890712); 安徽省自然科学基金项目(1808085J02); 中央高校基本科研业务费专项资金项目(WK2030000013); 中国博士后科学基金项目(2019M652177)

[†]通信作者: 张一飞, E-mail: ephy@ustc.edu.cn。